Title
EXPERIMENTS IN X-RAY HOLOGRAPHIC MICROSCOPY USING SYNCHROTRON RADIATION

Authors
Howells, M.R.
Iarocci, M.A.
Kirz, J.

Publication Date
1986-04-01

LBL-21364 c.2
Preprint

Lawrence Berkeley Laboratory
UNIVERSITY OF CALIFORNIA

Accelerator & Fusion Research Division

Submitted to Journal of the Optical
Society of America

EXPERIMENTS IN X-RAY HOLOGRAPHIC MICROSOCOPY
USING SYNCHROTRON RADIATION

M.R. Howells, M.A. Iarocci, and J. Kirz

April 1986

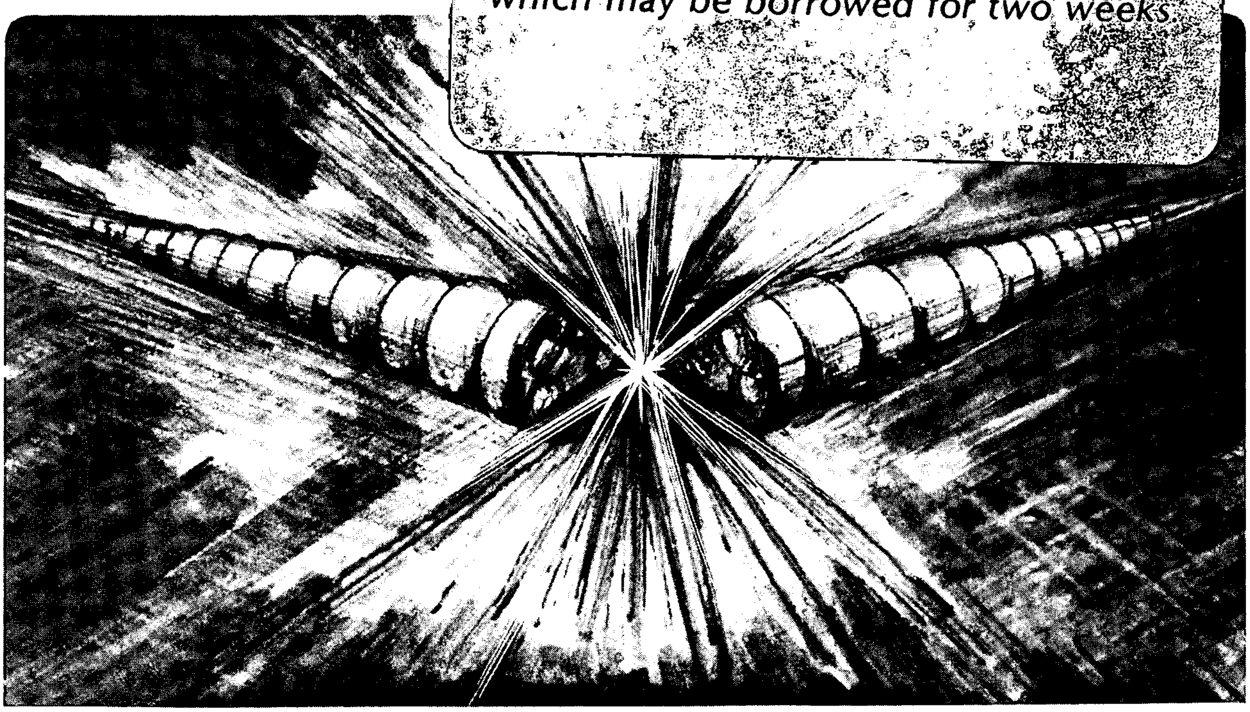

Prepared for the U.S. Department of Energy under Contract DE-AC03-76SF00098

LBL-21364

EXPERIMENTS IN X-RAY HOLOGRAPHIC MICROSCOPY USING SYNCHROTRON RADIATION

M.R. Howells* and M.A. Iarocci
National Synchrotron Light-Source
Brookhaven National Laboratory
Upton, NY 11973, USA

and

J. Kirz
Department of Physics
State University of New York
Stony Brook, NY 11794, USA

Lawrence Berkeley Laboratory
University of California
Berkeley, California 94720

April 1986

* now at the Center for X-ray Optics, Lawrence Berkeley Laboratory, University of California, Berkeley, CA 94720, supported by the U.S. Department of Energy under Contract Number DE-AC03-76SF00098.

ABSTRACT

We report on experiments in x-ray holographic microscopy using a storage ring x-ray source. Holograms of various simple objects in the size range 0.5 to 12 μm have been recorded using 0.4 keV x-rays and reconstructed using a He:Cd Laser (4416 Å). The reconstructed image characteristics are in line with expectations concerning resolution, signal to noise, field of view etc. In particular the transverse resolution in the best case was 1-2μm and exposure times were in the range 3-100 minutes.

EXPERIMENTS IN X-RAY HOLOGRAPHIC MICROSCOPY USING SYNCHROTRON RADIATION

by M. R. Howells* & M. A. Iarocci
National Synchrotron Light-Source
Brookhaven National Laboratory
Upton, NY 11973, USA

and J. Kirz**
Dept. of Physics
State University of New York
Stony Brook, NY 11794, USA

1. INTRODUCTION

During the last several years there has been a reawakening of interest in the possibilities of x-ray holographic microscopy.(1) This has been stimulated by the steady improvement in the quality of sychrotron radiation x-ray sources and a renewed optimism regarding the prospects for x-ray lasers.(2) In addition the successful demonstration of undulator sources of synchrotron radiation has led to rather firm projections of the quality of sources that will become available during the next one or two years. These projections lead us to expect sources with about a thousand times higher coherent x-ray power than current synchrotron sources and more than a million times higher than microfocus x-ray tubes.(3) Even higher values are technically within reach and still further technological developments are expected.(4)

* now at the Center for X-ray Optics, Lawrence Berkeley Laboratory, University of California, Berkeley, CA 94720

** J.S. Guggenheim Fellow, supported in part by the NSF under Grant #DMB-8540801

Against this background of source improvements we have begun to carry out a program of experiments aimed at demonstrating the feasibility of x-ray holographic microscopy at resolution levels superior to those previously demonstrated with x-ray tubes. We hope to verify the physical picture by which we presently believe we understand x-ray holography and rehearse the techniques which we will use in the future to make three dimensional images of biologically interesting objects such as cells. Our hope is that undulator sources will enable us to image wet, unstained cells in something close to their natural state and to push the resolution limit below the 1000Å level. Previous studies in x-ray holography, both theoretical[1,5-13] and experimental[14-17] have clearly demonstrated the need for sources of high spectral brilliance. Aoki et al.[15] were the first to use a synchrotron source for recording holograms, while Kondratenko and Skrinsky[9] provided the first evaluation of the coherent power available from storage ring sources. Detailed studies of holographic x-ray microscopy started with the work of Baez[5], Winthrop and Worthington,[6] Stroke,[7] and Rogers and Palmer.[8] The early history is reviewed by Aoki and Kikuta.[16]

In this paper we report a series of experiments in which objects in the size range 0.5-12 μm were holographed using x-rays of wavelength 31A. Preliminary results have been presented elsewhere.[18-19] We describe the storage ring - beamline configuration used as a source and the geometry of the holographic set-up. We discuss the hologram characteristics to be expected from such a system and we show holographic recordings for a number of samples. We also consider the reconstruction process and discuss results for several holograms that have been reconstructed with visible light. We pay special attention to the limitations of this type of reconstruction.

2. X-RAY SOURCE

Fig 1 shows the storage ring-beamline configuration. White soft x-rays originate in a bending magnet in the National Synchrotron Light Source (NSLS) 750 MeV electron storage ring. They are emitted as a horizontal fan which illuminates a grazing incidence toroidal diffraction grating monochromator in the U15 beamline. The electron beam is effectively the entrance slit of the monochromator. For present conditions the exit slit can give a beam of wavelength $\lambda = 31A$, bandwidth $\Delta\lambda = 0.1A$ and intensity 5×10^5 photons/sec/μm^2. This corresponds to a coherence length $(\lambda^2/\Delta\lambda)$ of about 1μm. The coherence solid angle for the storage ring source is given approximately by $\lambda^2/S_H S_V$ where S_H and S_V are the horizontal and vertical source sizes. For our case we have $S_H = 1.0$ mm, $S_V = 0.4$ mm so that we find $6 \times 15 \mu r^2$ for the (full width) coherence solid angle. Since the actual collected solid angle in U15 is about 10^5 times greater than this, the great majority of the collected photons must be discarded for experiments requiring coherence. This is conveniently done by use of a pinhole near the monochromator exit slit. The Airy cone of the pinhole thus becomes the illuminating beam for holography in similar fashion to the conventional laser-plus-spatial filter in visible light holography.

3. EXPERIMENT DESIGN

The storage ring and monochromator are parts of a windowless ultra high vacuum system and this is not convenient for microscopy. The pressure is therefore increased in two steps. The first one is from 10^{-10} torr to 10^{-7} torr by means of a thin (~1500 Å) aluminum contamination barrier which could withstand about 1 torr pressure difference. The second one is from 10^{-7} torr to the high pressure regime in the sample chamber via a silicon nitride window. The silicon nitride window is 200 x $200\mu m^2$ in area and about 1200 Å thick and can withstand atmospheric pressure. We are grateful to R. Feder and collaborators for providing the silicon nitride windows. The technique by which this group makes the windows is described in reference 20. Both windows are about 70% transmitting at 30Å. The outstanding properties of the silicon nitride window are the key to being able to cycle the sample chamber rapidly between atmospheric pressure and its operating pressure of 10^{-3} torr, which is suitable for soft x-ray transmission through the system.

The holographic geometry is shown in figure 2. We see that for the time being we are doing Gabor (in line) holography. We are working toward other holographic geometries but these have more stringent needs for optical components than Garbor geometry and are correspondingly less well developed. Our system allows various pinhole to plate (p) and sample to plate (q) distances and generally, for the small objects we are dealing with, the plate is in the far field of the sample (i.e. $q \gg w^2/\lambda$ where w is the sample width.) When this condition is satisfied the interference between the real and virtual images during reconstruction is minimised.

The practical realization of this holographic geometry involves a rack of interchangeable pinholes (of diameter d), a sample mount with x-y manipulation and an arrangement for viewing the sample in situ using a light microscope. The photographic plate is mounted in a modified McPherson vacuum spectrograph camera which allows recording of about a dozen holograms between plate changes. The photographic plates were chosen in accordance with the needs of Garbor holography to be of the highest possible resolution.
The dimensions of the system are adjustable in the ranges $100 < p < 500$ mm, $15 < q < 300$ mm and $0.5 < d < 25$ μm.

The specimen must be aligned with the spatially coherent x-ray beam which may be as small as 50μm, and is not normally visible to the naked eye even with the aid of a phosphor. The alignment is accomplished using a retractable, phosphor coated light pipe, coupled to a photomultiplier, which is able to detect the beam.

4. THEORY OF X-RAY HOLOGRAPHY

A great deal of thought has been devoted to understanding the physics underlying x-ray holography[1,5-13] and we do not wish to attempt a general discussion here. Instead we want to highlight a few issues which are relevant to understanding our present x-ray holograms and visible light reconstructions and which are important in the sense that they are involved in making projections into the future. As we can coherently illuminate only rather small (i.e. microscopic) objects, we are naturally lead to focus on the question of spatial resolution. For all forms of holography the transverse spatial frequencies f_x and f_y that are detected are limited according to the "grating equation" to

$$f_x \lesssim \frac{\theta_x}{\lambda} \quad ; \; f_y \lesssim \frac{\theta_y}{\lambda} \tag{1}$$

where θ_x and θ_y are the collection half angles of the beam diffracted from the sample. The highest longitudinal frequency f_z is given by

$$f_z \lesssim \frac{\theta^2}{\lambda}$$

where θ is the typical collection angle. Naturally there are questions concerning how "well" we must record the fringes at these limiting collection angles.

We now turn to a consideration of how the various experimental parameters determine the resolution achieved in Gabor holography:

4.1 Pinhole size and detector resolution:

These questions are discussed fully in the classic paper by Baez.[5] Baez argues that in Gabor holography each point on the sample contributes a Fresnel zone plate amplitude pattern at the detector. By computing the conditions under which the pinhole width and the detector grain size blur the rings of these zone plates he calculates resolution limits Δ_d and Δ_g due to pinhole diameter (d) and detector grain size (g) respectively:

$$\Delta_d = 0.61\, d \left\{\frac{q}{p}\right\}$$
$$\Delta_g = 1.22\, g \left\{1 - \frac{q}{p}\right\} \qquad (2)$$

4.2 The effect of the finite number of detected photons:

This issue is rather special to the case of holography with x-rays and has received some attention in the literature. The question is how many x-rays are needed to record a fringe pattern so that a feature of a given size can be reconstructed with a given signal to noise ratio (i.e. number of gray levels). In other words, the resolution predicted by equations (1) and (2) will not be achieved unless an adequate number of photons are detected and we wish to estimate that number. The practical limits on the number of detected photons are usually set either by the ability of the source to deliver coherent x-rays or by the sample's ability to tolerate them without morphological damage.

For the Fresnel Zone Plate amplitude pattern generated by each sample pixel at the hologram, the sample pixel size $\delta = 1.22\ \Delta r$[21] where Δr is the narrowest zone width of the zone plate pattern. Now the size of Δr is set by the detector resolution, $\Delta r > g$. To further define the zone plate pattern mentioned above we note that for working distance q (and dropping factors of 1.22) the pattern has radius $r_n \simeq \lambda q/2\delta$ and n rings where $n \simeq r_n/2\delta$. The number of detector elements participating in the imaging process (B) is thus given by

$$B = \pi r_n^2/\delta^2 = \pi q^2\lambda^2/4\delta^4 \qquad (3)$$

We show elsewhere[22] that the smallest total number of x-rays (N_T) that can encode the required positional and gray level information for N_o sample pixels is given by

$$N_T \simeq B \quad R^{\frac{2N_o}{B}} \quad . \qquad \text{where } R = \frac{4B^2\delta\ell}{\pi^2 q} \qquad (4)$$

and ℓ is the number of gray levels.

We need not enquire too much about R since $(R)^{2N_o/B}$ in equation (4) can be made arbitrarily close to unity by choosing $2N_o/B$ sufficiently small. This latter condition, that the number of detector pixels be much larger than the number of sample pixels, is intuitively reasonable.[1] Examination of (4) shows that B/N_o needs to be in the range a few tens to a few hundreds for practical cases. This is similar to the number of recorded photons esti- mated by Mueller and Jorna[10] and by Morris[23] as necessary for detec- tion of each sample pixel with reasonable miss and false alarm rates. Assuming the R term in (4) is close to unity, the remaining messages are firstly that N_T becomes approximately equal to B and secondly that the scaling law for N_T with δ is $N_T \propto \delta^{-4}$, other variables being kept fixed. We discuss the scaling law elsewhere.[22] The value of B in these experiments can be found roughly from table I (hologram area divided by film resolution element area) and compared with the number of x-rays actually used. We notice that in all cases we have used more than a thousand times more than the minimum number of x-rays specified by (4). We do not find this suprising and attribute it mainly to detector inefficiencies and the fact that our method of reconstruction is highly wasteful of information compared to an optimised numerical reconstruction method. We plan to address these matters in future experiments.

4.3 Aberrations:

The aberration coefficients of holographic systems have been calculated up to fourth order in the aperture co-ordinates by Meier.[24] The calculation includes the effect of recording at wavelength λ_1 and reconstructing at wavelength λ_2. In Gabor holography with $\lambda_1 \neq \lambda_2$, the aberrations of the axial point are all zero except for spherical aberration. This latter aberration is always present, unless the hologram is scaled by a factor λ_2/λ_1. For cases of interest to us this factor is about 200 so physical scaling is difficult. In our experiments we did not scale the holograms and we obtained reasonable images. The amount of resolution blurring due to spherical aberration for our holograms is discussed in section 7 and given quantitatively in table II.

We note that aberrations can be eliminated altogether in a numerical reconstruction.

4.4 Resolution effects due to imperfect source coherence:

This is an effect that allows the formation of good contrast fringes over only part of the hologram area. The effect on the resolution is via restriction on the effective collection angles in equation (1), and has been analyzed by Solem and Chapline[1]

5. EXPERIMENTAL RESULTS

Figs 3-5 show examples of holograms and reconstructions made at Brookhaven with the apparatus described in section 3. The detailed parameters of both recording and reconstruction are given in Tables I and II.

6. DISCUSSION OF THE HOLOGRAM RECORDINGS

The most obvious feature of the recordings is the very uneven illumination of the sample as shown by the dark diffuse spot on the photographic plate, which is the nominally circular Airy cone of the illuminating pinhole. It is apparent that our pinholes have considerable departures from roundness. From the shape of the illuminated spot we can picture the coherence function and guess the spatial coherence limits in effect. This uneven reference beam is not necessarily bad because the strengths of the sample Fourier components usually diminish with increasing frequency (angle) and the weaker reference beam at large angles tends to match it.

The theoretical basis for understanding the form of a Gabor hologram of a small particle has been given by Tyler and Thompson.[25] They derive analytical expressions for the holograms of two simple shapes: the parallel sided strip and the circular disc. Illumination is assumed to be by a plane wave of uniform intensity. Our experiments roughly correspond to the above ideal cases and we do, indeed, observe fringe patterns which are in qualitative agreement with the ones we calculate using the method of reference 25. Considering the approximate way in which we know the sample geometry and the coherence and intensity distribution of the illuminating beam we do not expect quantitative agreement.

The holograms in Figs. 3 and 5 were taken with the lower resolution Kodak 131 film and resulted from our earliest attemps to make x-ray holograms using the U15 beamline as a source. The main thrust of these experiments was to demonstrate that an apparatus made with ordinary engineering methods would have the mechanical and thermal stability to record x-ray interference fringes and to develop our technique generally. We also hoped to imitate the ideal objects and geometries used in calculations as closely as possible and compare theory and experiment. The holograms shown required exposure times of a few minutes and, indeed, demonstrate that we have sufficient overall stability. The number of fringes is apparently somewhat greater than in earlier experiments and certainly provides a recording that can be reconstructed. Three factors appear to be involved in limiting the number of fringes. First, the fringe frequency in figure 3(a) is about 1000 cycles/mm which is not far from the photographic plate cutoff frequency of 1250 cycles/mm quoted by the manufacturer. Examination of the grain structure in figure 3(a) shows that it is questionable whether the quoted cutoff frequency could be achieved. Second, the signal to noise ratio is diminishing as the strength of both scattered and transmitted beams becomes weaker as one goes away from the center of the field. Third, we know that the good spatial coherence region extends only over a diameter equal to about 26%[26] of the diameter of the first minimum of the Airy pattern and we might expect to encounter partial coherence effects outside this. We do know that our temporal coherence is > 200 waves and is therefore not involved in determining the fringe count.

For the hologram in fig 4 we made extra efforts to get high resolution involving in particular the use of a nominal 1μm pinhole and the higher resolution Agfa 8E56HD film which has a quoted cut off frequency of about 5000 cycles/mm. There are great penalties in count rate involved in the quest for high resolution. The Agfa film is about a factor of twenty slower than the Kodak. In addition, the use of a two-fold smaller diameter pinhole leads to a four fold loss in x-ray transmission and a four-fold increase in the film area illuminated by the Airy cone of the pinhole. This is a 320-fold loss of overall speed. We mitigated this somewhat by a reduction in the working distance. One can see from Table II that our attempts at higher resolution were foiled by aberrations coupled with signal to noise problems that are difficult to quantify.

From the parameters given in Table I we can estimate the exposure on the holograms as follows: The reference illumination is effectively the central part of the Airy pattern from the pinhole source. Its diameter is comfortably larger than the useful hologram size (see Table I). The average intensity of the reference illumination is crudely estimated as the total number of photons divided by the area of the Airy disk. The object intercepts a small fraction of these x-rays. Assuming a black-disk model for the scattering, the elastic cross section is equal to the geometrical area of the object. This model allows us to estimate the number of photons scattered, and based on the observed area of fringes on the hologram, to calculate the average illumination generated by these photons over that area. These estimates are given in Table I. We find that the ratio of object illumination and reference illumination is in the range 1/18 - 1/180. The amplitudes that interfere to generate the fringes are in the ratio $1/\sqrt{18}$ - $1/\sqrt{180}$, consistent with the observed modulation, or average fringe visibility, which is in the 7-25% range.

7. DISCUSSION OF THE RECONSTRUCTIONS

The main result of the experiments is that the holograms could be made with x-rays and reconstructed with visible light to give a final image resolution of about 1 μm. We now try to analyze the influence of the experimental parameters on this result and discuss the implications for the future.

The paraxial optics of the system do indeed obey the known conjugate relations but some important features emerge. First, the parameter choices that give reasonable exposure times for the hologram lead to inconveniently small conjugates for reconstruction. In the present cases the reconstructing source to hologram distances are in the range 0.55-1.1 mm as shown in Table II. Another noticeable feature is the virtual absence of holographic magnification. This is expected[28] but it means that we are depending almost entirely on the light microscope to get magnification when we view and photograph the final image. The reason why this is hard to avoid is as follows: suppose we try to choose a value of the reconstruction source to hologram distance (z_c) to get high magnification. This would be near the value at which the magnification tends to infinity and the real image jumps to the other side of the hologram. In this case we find z_c is $(\lambda_1/\lambda_2)(1/z_1 + 1/z_R)^{-1}$. Since λ_1/λ_2 is a small number this distance is small and the angle subtended by the hologram is larger than one can deliver with a laser-plus-pinhole. This general situation can only be improved by scaling up the hologram.

The most significant conclusions discernable from the reconstruction parameters given in Table II concern the various resolution limits. There appears to be a contradiction between the achieved resolution values and the quoted aberration limited values which are larger in some cases. The explanation is that the aberration limits are calculated for a fringe system that fills the entire hologram width (w in the Table). In practice the fringes from a particular pixel often fill only part of the hologram leading to a lower aberration blur width. In fact for spherical aberration, even a factor two drop in the width of the fringe system leads to a factor eight drop in the blur width as explained in the footnote to Table II. Even allowing for this, however, it is clear from Table II that we cannot expect to get far into the submicron range of resolution using the present strategy of reconstructing an original Gabor hologram with visible light. Again, the situation could be improved by scaling up the hologram. The resolution limit would then be set by the fidelity of the "enlarger" that would be used. With standard visible/UV techniques one can imagine achieving resolutions of about 0.2-0.3 μm by these means. It could well be that there are applications in this range although the corresponding longitudinal resolution [equations (1)] is ~10 μm and in view of the penetrating power of soft x-rays this corresponds to two dimensional imaging only.

We can also study the reconstructions to see how they conform to the theoretical results of Tyler and Thompson.[25] One of the main conclusions of these workers is that for their examples the image plane contains, apart from the image, another hologram which arises from the virtual image (as the object) and the reconstructing beam (as the reference). The new hologram is similar to the original one apart from being scaled up on account of the larger object to hologram distance. For our reconstructions we do indeed observe this second hologram [see for example fig 4(b)].

8. FUTURE STRATEGIES

The broad picture of the foregoing analysis is that x-ray holography using Gabor geometry and visible light reconstruction of the original hologram breaks down around the 0.5-1 μm resolution level. The breakdown is due to the combined effect of aberrations, detector resolution and the diffraction limit inherent in visible light reconstruction. In order to achieve resolutions much better than 1 μm there are at least two general strategies that are possible.

The first is to continue with the Gabor method (or any other Fresnel geometry), choose a working distance long enough to satisfy the considerations of section 4.2 and short enough to give a reasonable temporal coherence requirement, and use high resolution x-ray resist as a detector.[20] The patterns recorded in this way will be too fine to be reconstructed with visible light and some approach involving electron microscopy will be needed. If this can be implemented with adequate fidelity then there are various ways to get to the final image. The simplest is visible light reconstruction of the magnified hologram. Numerical reconstruction offers opportunities for superior optimization of the process in return for correspondingly greater effort.

The second strategy for higher resolution imaging is to use Fourier transform geometry. This promises to allow the continued use of photographic film and visible light reconstruction, or electronic detectors with computer reconstruction. The main challenge is to form the reference source. Whether this is a point or an extended aperture, its structural detail sets the limit to the resolution.

Both these approaches appear to be promising and we are optimistic about the prospects for high resolution experiments with the new generation of soft x-ray sources. As our technique improves and we begin to image dense (as opposed to sparse) objects and as our resolution goals move toward smaller pixel sizes we expect to encounter various new problems and limits. These will be due to speckle,[27] radiation damage and the tomographic limit arising from our use of a single view. Experience will show how far we can go in overcoming these problems. However, we do anticipate using multiple views and we expect to develop ways of making optimum use of the detected information so as to keep the x-ray dose to the sample as low as possible. We believe that efficient incorporation of prior knowledge can help in this effort. Finally, when the unavoidable damage limit is reached, our only recourse will be to use flash illumination.[1]

9. CONCLUSION

We have described a series of x-ray holographic experiments which closely parallel the classical technique of visible light holography using photographic film. The reconstructed images achieved a resolution of ~ 1 μm. These experiments were analysed in terms of their intelligibility using conventional holographic theory and their potential for development toward higher resolution. The results are consistent with theoretical expectation. For improvement in resolution either Fourier transform geometry or the use of high resolution resist detectors is suggested.

ACKNOWLEDGEMENTS

The authors wish to acknowledge the assistance and advice of the creators of the U15 beamline especially H. Rarback and J. Kenney and valuable discussions with G. Chapline, R. Feder, C. Jacobsen, D. Sayre, J. Solem, B.J. Thompson.

The National Synchrotron Light Source is supported by the Department of Energy under Contract #DE-AC02-76CH00016.

REFERENCES

(1) J.C. Solem and G.C. Baldwin, "Microholography of living organisms", Science 218, 229(1982), J.C. Solem and G.F. Chapline, "X-ray Bio-microholography", Opt. Eng. 23, 193(1984)

(2) D.L. Matthews et al "Demonstration of a Soft X-ray Amplifier" Phys. Rev. Lett 54, 110(1985) and M.D. Rosen et al, "Exploding Foil Technique for Achieving a Soft X-ray Laser", Phys. Rev. Lett. 54, 106(1985)

(3) M. Howells and J. Kirz, "Coherent Soft X-rays in High Resolution Imaging", in "Free Electron Generation of Extreme UV Coherent Radiation" (AIP Conf. proc. Vol.118), J.M.J. Madey & C. Pellegrini eds. 1984 p.85.

(4) D. Attwood, K. Halbach, K-J Kim, Tunable, Coherent X-rays, Science 228, 1265(1985)

(5) A.V. Baez, "A study in Diffraction Microscopy with Special Reference to X-rays", J. Opt. Soc. Am. 42, 756(1952)

(6) J.T. Winthrop and C.R. Worthington, "X-ray Microscopy by Successive Fourier Transformation", Phys. Lett. 15, 124(1965)

(7) G.W. Stroke, "Attainment of High Resolutions in Image Forming X-ray Microscopy with 'lensless' Fourier-Transform Holograms and Correlative Source Effect Compensation" in Optique des Rayons X et Microanalyse, Hermann, Paris(1966) p.30

(8) G.L. Rogers and J. Palmer, "The Possibilities of X-ray Holographic Microscopy", J. Microsc. 89, 125(1969)

(9) A.M. Kondratenko and A.N. Skrinsky, "Use of Radiation of Electron Storage Rings in X-ray Holography of Objects", Opt. Spectrosc. 42, 189(1977)

(10) R.K. Mueller and S. Jorna, "Intensity requirements in X-ray Holography at 1Å", Appl. Opt. 16, 525(1977) and in Applications of X-ray Lasers, Physical Dynamics Report PD-LJ-76-132(1976), sec 7.

(11) A.M. Kondratenko and A.N. Skrinsky, "X-ray Holography of Micro-objects" in Optical Information Processing, Vol II, ed. E.S. Barrekette et al., Plenum, NY, 1978 P.1

(12) V.V. Aristov and G.A. Ivanova, "On the Possibility of Using Holographic Schemes in X-ray Microscopy", J. Appl. Cryst. 12, 19(1979)

(13) V.V. Aristov, G.A. Bashkina, and A.I. Erko, "Holography of Micro-Objects in Soft X-rays", Opt. Comm. 34, 332(1980)

(14) S. Kikuta, S. Aoki, S. Kosaki, and K. Kohra, "X-ray Holography of lensless Fourier-transform type", Opt. Comm. 5, 86(1972)

(15) S. Aoki, Y. Ichihara, and S. Kikuta, "X-ray Hologram obtained by Using Synchrotron Radiation", Jap. J. Appl. Phy. 11, 1857(1972)

(16) S. Aoki, and S. Kikuta, "X-ray Holographic Microscopy", Jap. J. Appl. Phy. 13, 1385(1974)

(17) B. Reuter and H. Mahr, "Experiments with Fourier Transform Holograms using 4.48 nm X-rays", J. Phys. E9, 746(1976)

(18) M.R. Howells, "Possibilities for X-ray Holography using Synchrotron Radiation", in X-ray Microscopy, Ed. by G. Schmahl and D. Rudolph, Springer, Berlin, 1984 p.318

(19) M.R. Howells et al. "X-ray Holographic Microscopy Experiments at the Brookhaven Synchrotron Light Source", in Science with Soft X-rays, F.J. Himpsel and R.W. Klaffky eds. Proc. SPIE 447, 193(1984)

(20) R. Feder, D. Sayre, "Recent Developments in X-ray Contact Microscopy", Ann. NY. Acad. Sci. 342, 213(1980)

(21) O.E. Myers Jr., "Studies of Transmission Zone Plates", Am. J. Phys. 19, 359(1951)

(22) Optical Society of America Topical Meeting on "Short Wavelength Coherent Radiation: generation and applications" Monterey 1986: Proceedings to be published.

(23) G.M. Morris, "Scene Matching Using Photon Limited Images", J. Opt. Soc. Am. A, 1, 482(1984)

(24) R.W. Meier, "Magnification and Third Order Aberrations in Holography", J. Opt. Soc. Am. 55, 987(1965)

(25) G.A. Tyler and B.J. Thompson, "Fraunhofer Holography Applied to Particle Size Analysis: a Reassessment", Optica Acta 23, 685(1976)

(26) M. Born and E. Wolf, "Principles of Optics", Pergamon, Oxford, 6th ed: 1980, equation (31) in section 10.4

(27) E. Spiller, Proceedings of the Workshop on "Applications of Laboratory X-ray lasers", Ed. by N. Ceglio, Asilomar, February, 1985

(28) M.R. Howells, M. Iarocci, J. Kenney, H. Rarback, R. Rosser and W. Yun. "Application of Holography to X-ray Imaging", Proc. SPIE. 523, 347(1985)

(29) G.C. Bjorklund, S.E. Harris, and J.F. Young, "Vacuum Ultra-violet Holography", Appl. Phys. Lett. 25, 451(1974)

TABLE 1 HOLOGRAM PARAMETERS

		1. single wire	2. asbestos fibres	3. glass spheres
object size (μm)		12.5	0.5–2.0	3–10
Magn of 8 1/2x11 photo		500	500	500
recording wavelength (Å)	λ_1	31	31	31
reference source size (μm)	d	2	1	2
source-plate distance (mm)	z_R	173	144	173
sample-plate distance (mm)	z_1	58	29	58
recording medium		Kodak 131-01	Agfa 8E56HD	131-01
quoted res'n of medium (μm)	g	0.8	0.2	0.8
Hologram width (μm)*	w	300	300	350
exposure time (min)		3	44	3
total # of photons$\times 10^9 \pm 300\%$		.6	3	1
D_{Airy} (μm)		650	1100	650
reference illumination on hologram (x-rays/μm^2)		1800	3000	3000
object area μm^2		12.5x400	1x20	100
flux incident on object (x-rays/μm^2)		4000	5000	6700
x-rays scattered by object		2×10^7	10^5	7×10^5
fringe-area on hologram due to single object (μm^2)		300x300	60x60	80x80
illumination on hologram from object-wave (x-rays/μm^2)		220	28	100
object beam intensity/ reference beam intensity		1/18	1/180	1/30

* Width over which fringes are discernable by eye

TABLE II RECONSTRUCTION PARAMETERS

	1. Single wire	2. Asbestos fibers	3. Single fiber**	4. Glass speres
reconstructing wavelength (A) λ_2	4416	4416	4416	4416
recon. source-holog dist (mm) z_c	1.05	0.90	0.55	1.1
hologram-real image dist (mm) z_3	1.5	0.40	0.48	1.4
magnification of recon. image M_R	3.6	1.7	2.4	3.4
magn of 35mm photo of image M_P	50	100	200	100 200
recon source size (μm)	2	0.5	1.0	1.0
sph. ab: full width for half the rays (μm)*	2	7	2	3
Resolution limit due to diffraction (eqn 1) (μm)	.6	.6	.9	1.0
Baez eq source size limit (μm) Δ_p	.4	.12	.12	.4
Baez eq grain size limit (μm) Δ_g	.6	.2	.2	.6
achieved transverse res'n (μm)	1-2	1-2	1-2	1-2

* Since the spherical aberration term in the optical path function is proportional to the aperture co-ordinate (r) to the fourth power, the transverse ray aberration is proportional to r^3 and the ray density follows an r^{-3} law. Thus half the rays have aberrations less than one eighth that of the marginal ray.

** The hologram in 3. is the same as in 2. We are considering here a different reconstruction during which only part of the hologram was illuminated by the reconstruction source.

Figure captions

1. Layout of the storage ring/beamline system used as an x-ray source for x-ray holographic recordings.

2. Layout and notation for the Gabor holographic geometry employed in the present experiments. Actual values of the parameters are given in Table 1.

3 (a) Hologram of a single 10μm steel wire. (b) reconstruction using visible light. (Column 1 in tables I and II)

4 (a) Hologram of several ammosite asbestos fibers, diameter 0.5-2.0μm (b) reconstruction using visible light. (column 2 in tables I and II) (c) reconstruction of part of the hologram in 5(a) using visible light (column 3 in table II)

5. (a) Hologram of clusters of glass spheres 3-10μm diameter (column 3 in table I) (b) reconstruction using visible light (column 4 in table II)

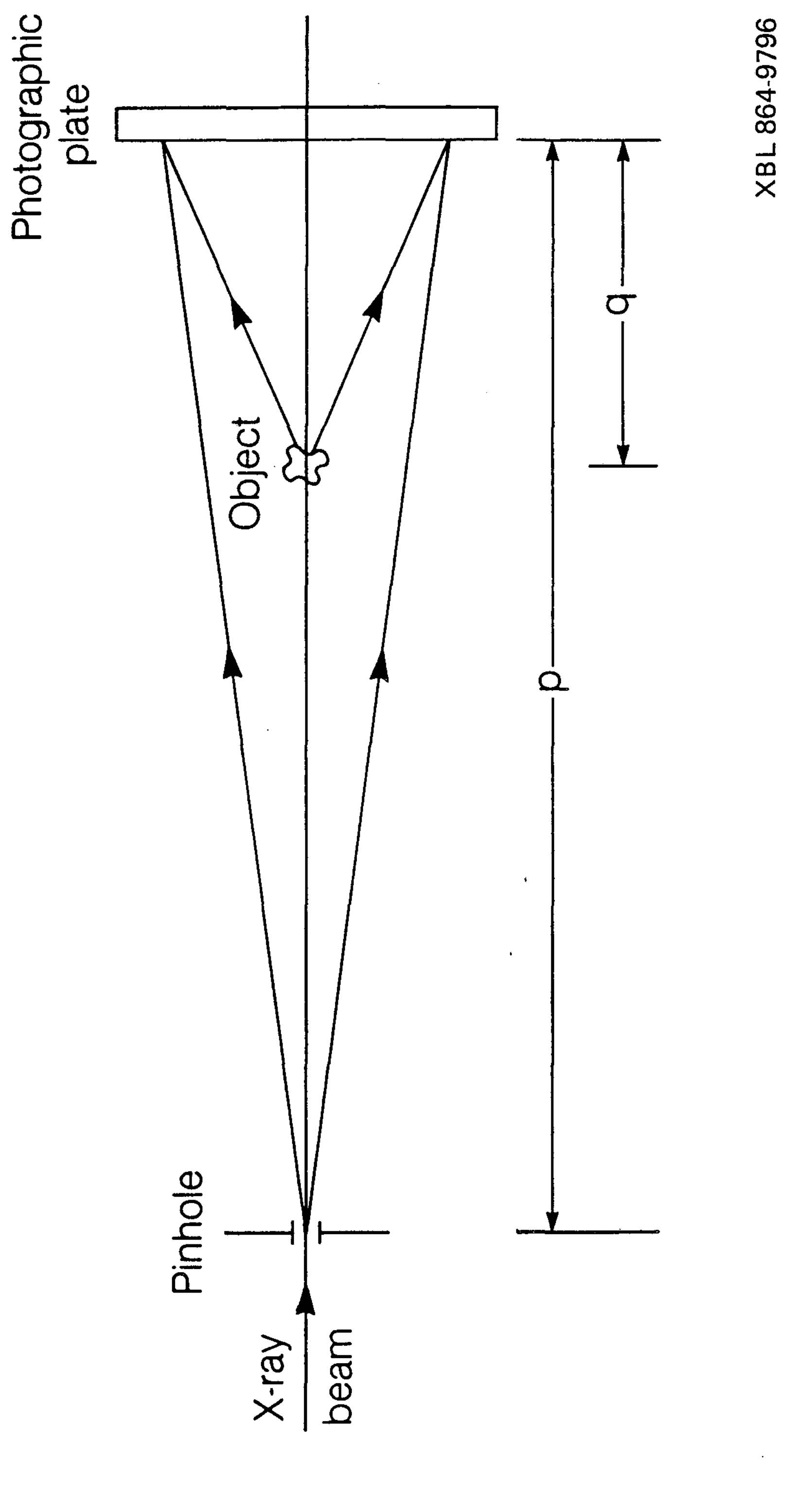
Photographic plate
Object
q
p
Pinhole
X-ray beam
XBL 864-9796

Fig. 2

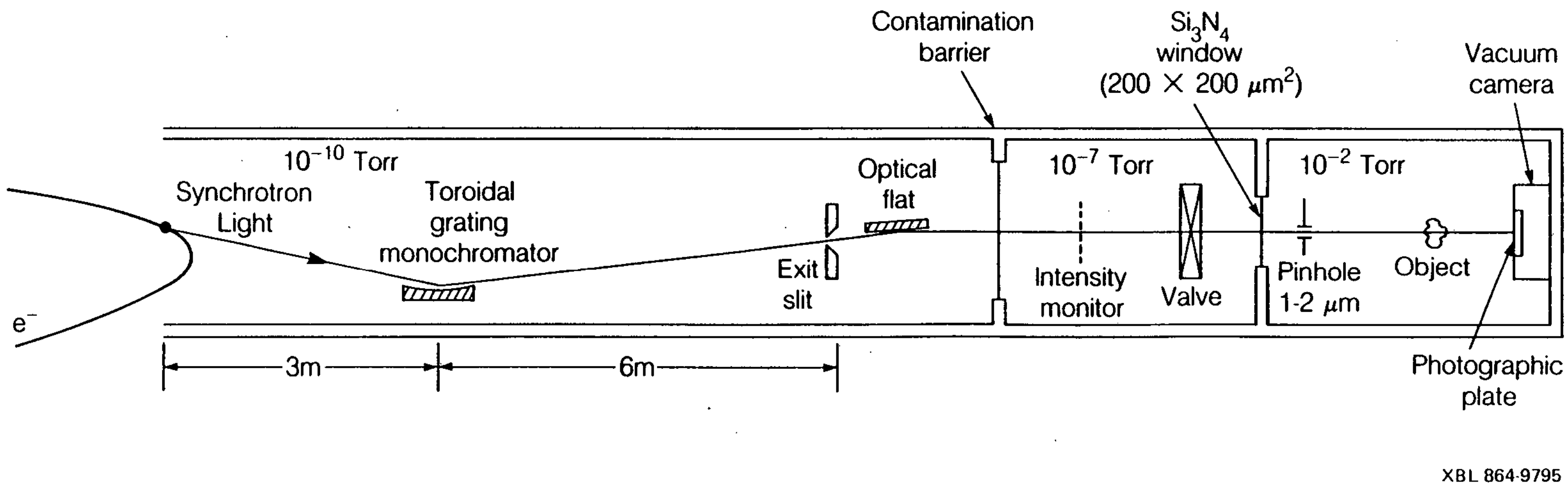
Contamination barrier
Si_3N_4 window
(200 × 200 μm^2)
Vacuum camera
10^{-10} Torr
10^{-7} Torr
10^{-2} Torr
Synchrotron Light
Toroidal grating monochromator
Optical flat
Exit slit
Intensity monitor
Valve
Pinhole 1-2 μm
Object
e⁻
3m
6m
Photographic plate
XBL 864-9795

Fig. 1

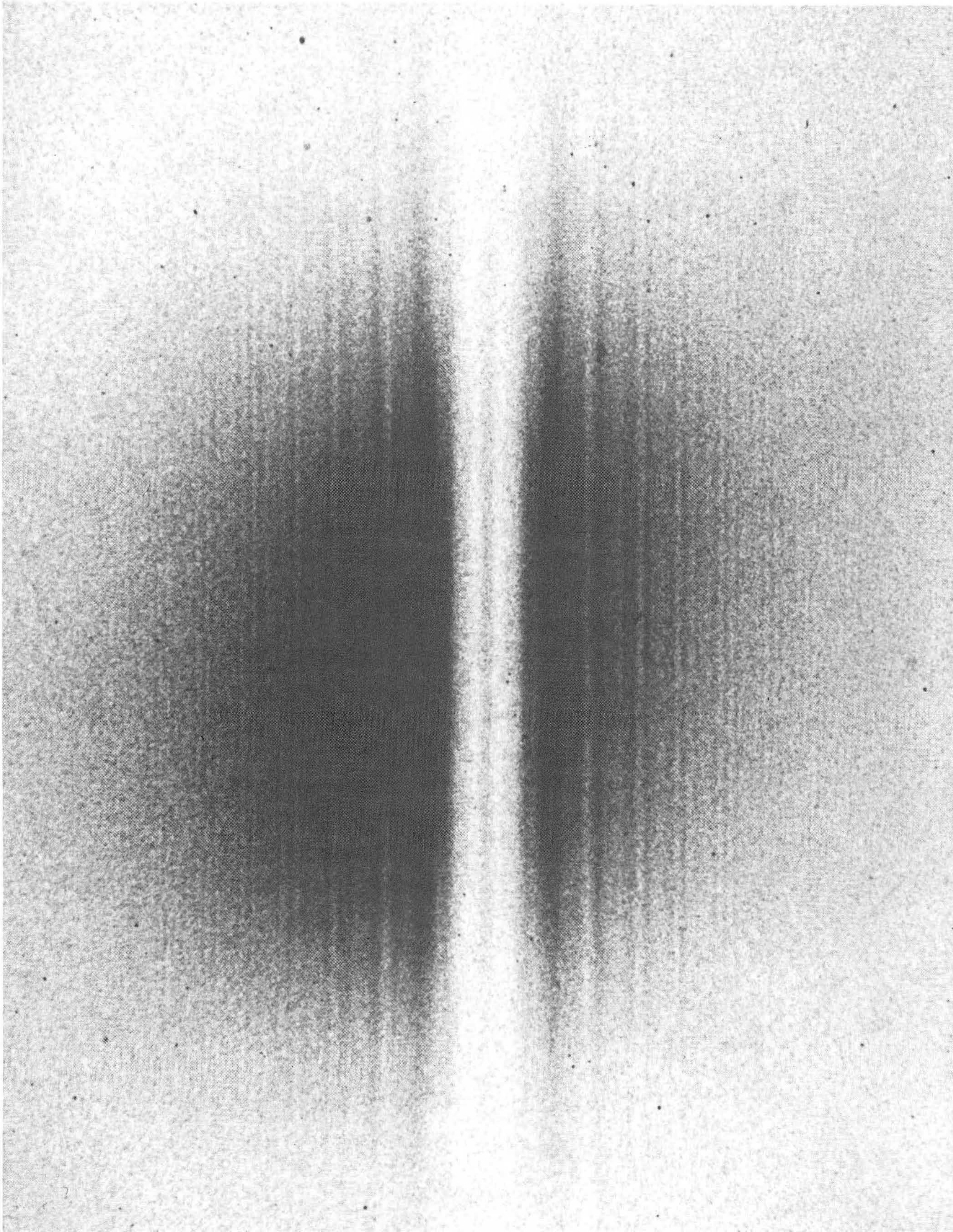

Fig. 3(a)

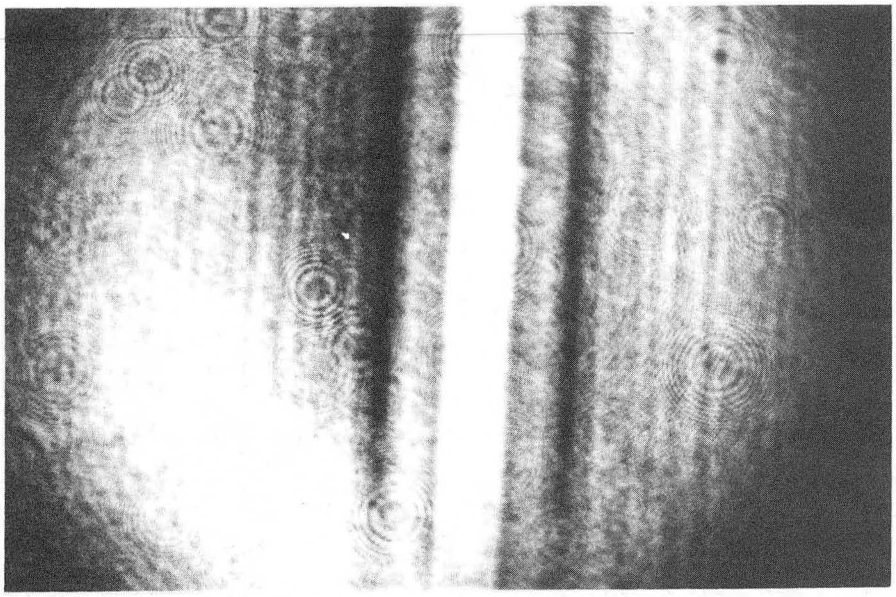

Fig 3(b)

Fig. 4(a)

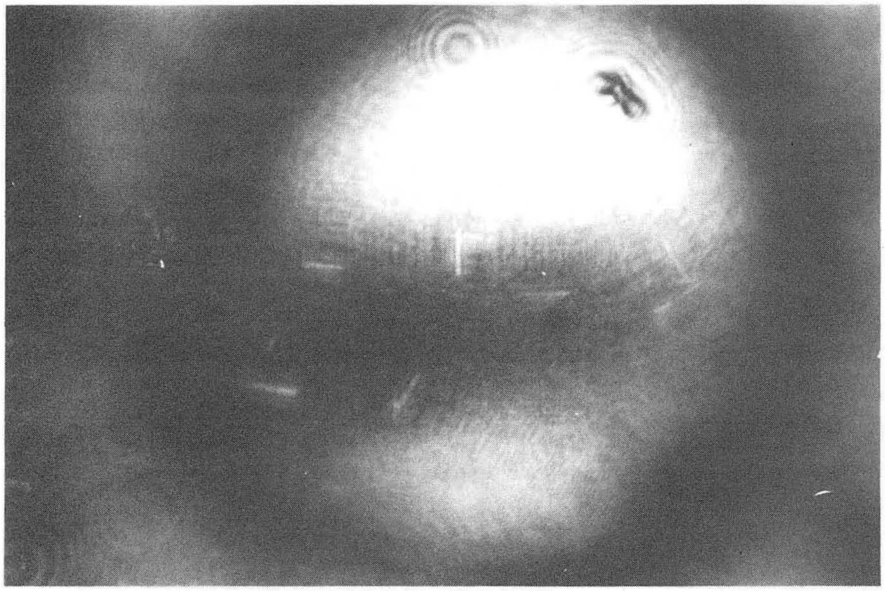

XBB 853-2089

Fig 4(b)

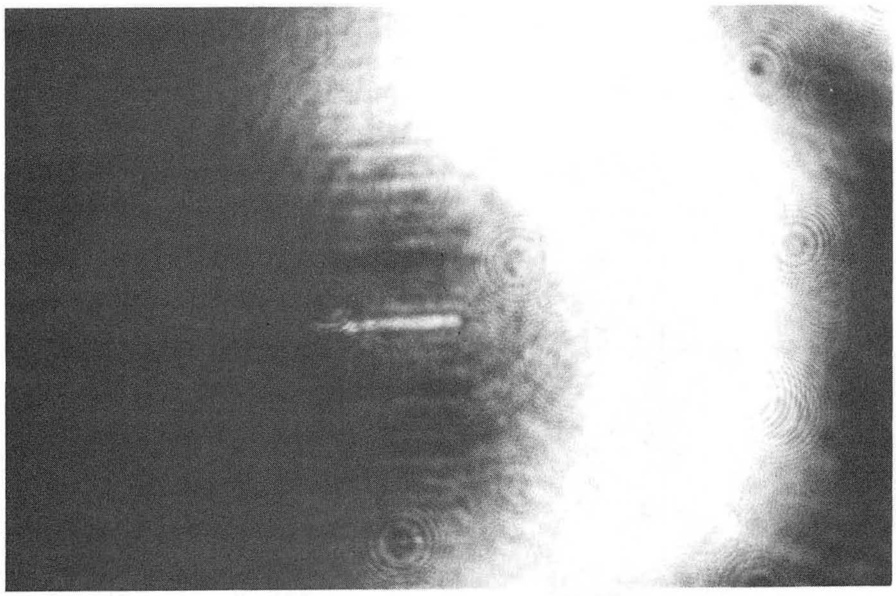

Fig 4(c)

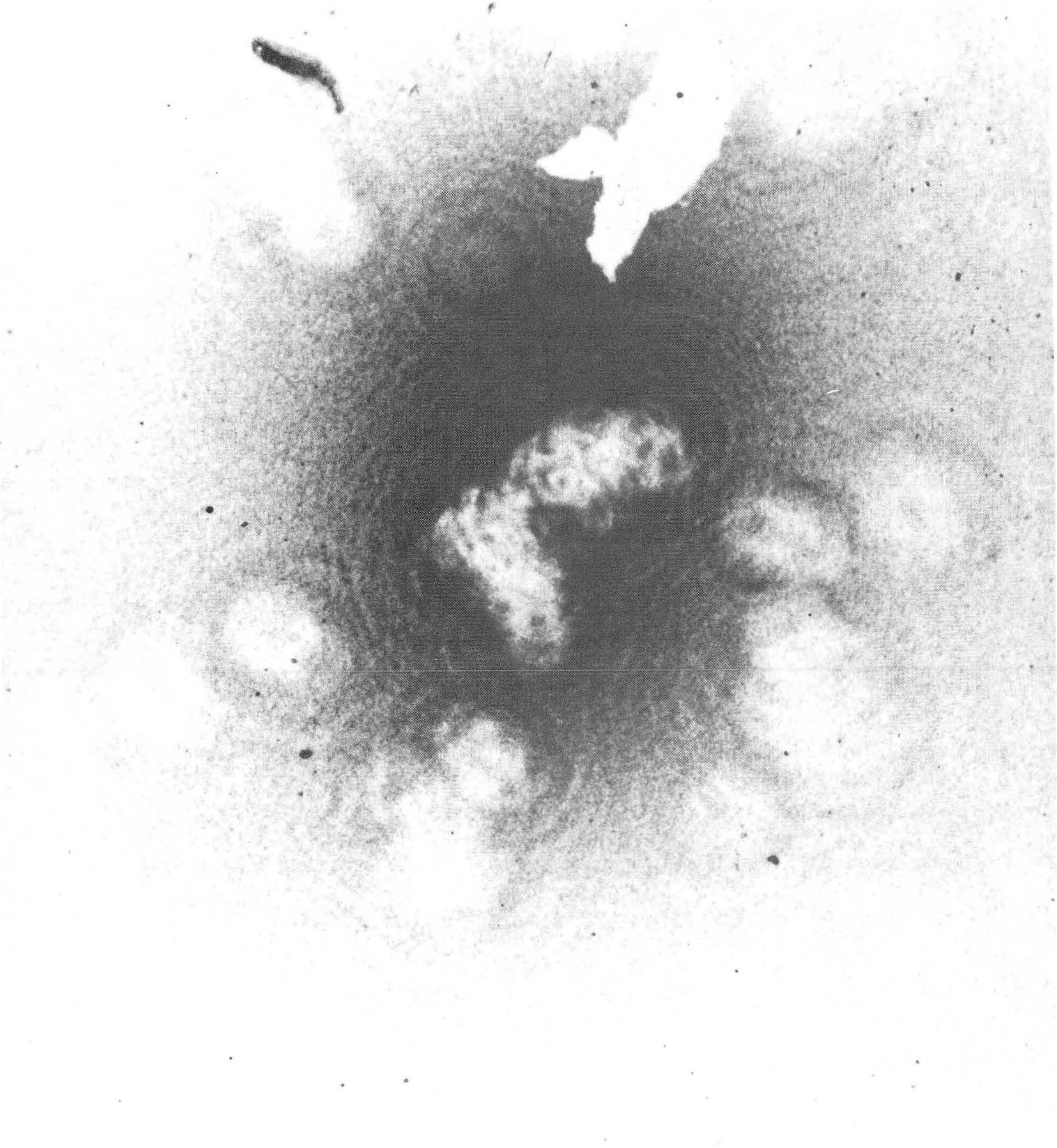

Fig. 5(a)

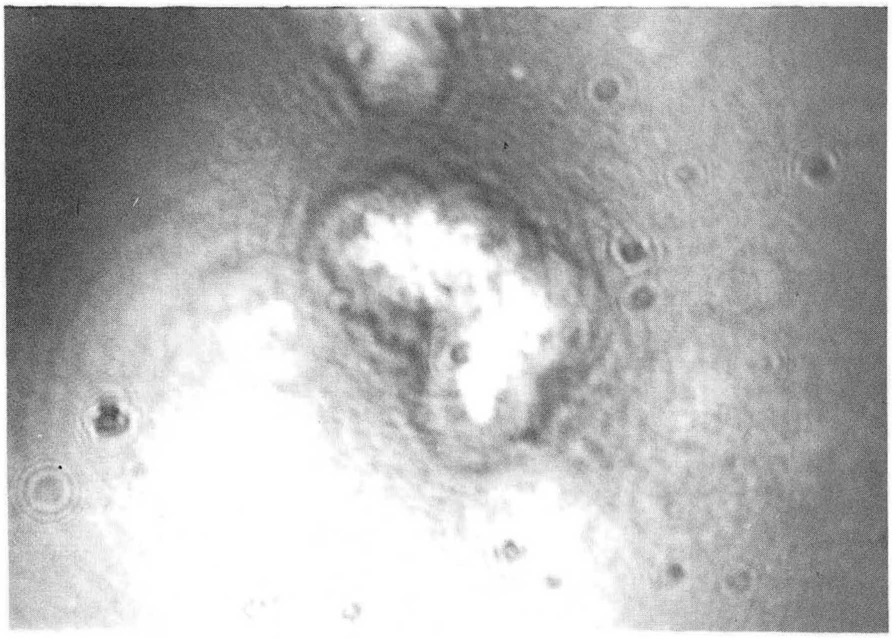

Fig 5(b)

LAWRENCE BERKELEY LABORATORY
TECHNICAL INFORMATION DEPARTMENT
UNIVERSITY OF CALIFORNIA
BERKELEY, CALIFORNIA 94720